Wideband Decoupled Millimeter-Wave Antenna Array for Massive MIMO Systems

Zhang, Yi-Ming ; Yao, Ming; Zhang, Shuai

Published in:
I E E E Antennas and Wireless Propagation Letters

DOI (link to publication from Publisher):
10.1109/LAWP.2023.3291175

Publication date:
2023

Document Version
Accepted author manuscript, peer reviewed version

Wide-Band Decoupled Millimeter-Wave Antenna Array for Massive MIMO Systems

Yi-Ming Zhang, *Member, IEEE*, Ming Yao, and Shuai Zhang, *Senior Member, IEEE*

***Abstract*—This letter presents a wide-band decoupling method to suppress the mutual coupling among dual-polarized millimeter-wave antenna arrays for massive multiple input multiple output systems. With the contribution of the proposed decoupling structure, the coupling between elements can be reduced by confining the electromagnetic field propagating along the array aperture plane. An 8×8 millimeter-wave dual-polarized antenna array loading with the proposed decoupling structure is further developed. The full-wave simulated results show that an isolation level of over 25 dB can be achieved from 24.3 GHz to 29.7 GHz. The measured results are fixed well with the simulated results, denoting that the proposed scheme is effective and valuable for millimeter-wave large-scale antenna array applications.**

***Index Terms*—Millimeter-wave antenna, massive multiple input multiple output antenna, decoupling dielectric stub.**

I. INTRODUCTION

MASSIVE multiple input multiple output (MIMO) is considered a key technology for future wireless communications, since it enables hundreds of steerable beams to specified directions for serving individual users simultaneously. However, antenna coupling in a massive MIMO antenna array is an issue since it would severely degrade the coverage area and scanning performance of the antenna systems, for instance, enhancing active impedance matching responses, increasing the error rate of wireless communication, and bringing nonlinear distortion on power amplifiers. Thus, mutual coupling suppression is of great significance to array systems [1]-[14].

Antenna array decoupling for Sub-6 GHz applications has been widely studied in recent years [1]-[9]. As for millimeter-wave (MMW) applications, achieving decoupling through a specified design at radiating aperture is more popular since limited physical space greatly confines the decoupling operation at the feeding layer [10]-[14]. In [10], a decoupling method using vias embedded in dielectric resonator antennas was proposed for MMW two-element arrays. In [11], air holes in the substrate layer were inserted in between MMW elements to suppress the coupling to lower than -20 dB. In [14], a current-cancellation method was reported for MMW antenna array decoupling, by loading branches between patches. The aforementioned methods are effective for specified arrays, however, still have limitations on decoupling bandwidth, array scale, and dual-polarization operation.

This letter provides a decoupling scheme for MMW massive MIMO arrays. Note that the proposed scheme is an improvement of the previous work reported in [7] where a single-layer decoupling stub is proposed. Compared to the published work, the decoupling bandwidth of the proposed one is significantly enlarged. An 8×8 MMW dual-polarized decoupled array is fabricated and tested. Although the proposed decoupling structure requires an additional profile of around $1.1\lambda_0$ at the center frequency of 26.75 GHz, it is still acceptable since the physical height of the decoupling structure is around 12 mm. Both simulated and measured results are given to demonstrate the performance of the proposed scheme.

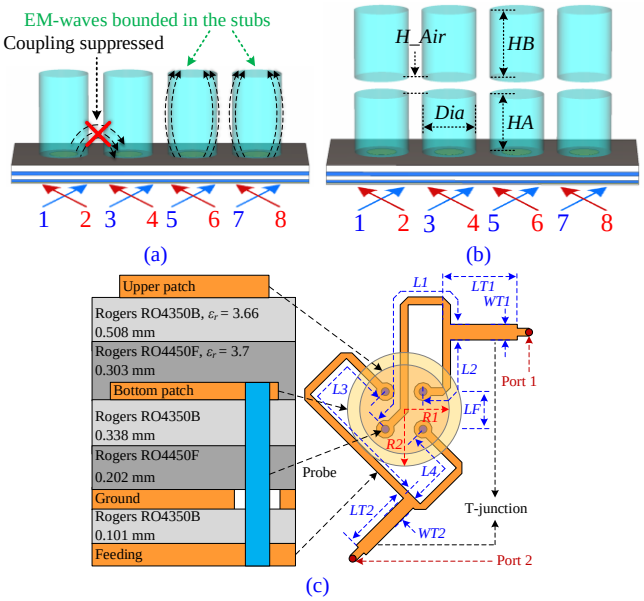

Fig. 1. Configurations of dual-polarized 1×4 patch antenna arrays with (a) single-layer and (b) dual-layer decoupling stubs. (c) Physical layout of the dual-polarized MMW antenna element.

II. ANALYSIS AND SIMULATION

A. Proposed scheme

Shown in Fig. 1(a) is a 1×4 dual-polarized patch antenna

This work was partially supported by Huawei project of "5G mmWave Decoupling Array" and the Guangdong Basic and Applied Basic Research Foundation under Grant 2023A1515011412. (*Corresponding author*: *Shuai Zhang*.)

Yi-Ming Zhang is with the School of Electronics and Information Technology, and Guangdong Provincial Key Laboratory of Optoelectronic Information Processing Chips and Systems, Sun Yat-Sen University, Guangzhou 510006, China. (email: zhangyim9@mail.sysu.edu.cn).

Ming Yao and Shuai Zhang are with the Antenna, Propagation and Millimeter-wave Systems (APMS) Section, Department of Electronic Systems, Aalborg University, 9220 Aalborg, Denmark (e-mail: mingya@es.aau.dk, sz@es.aau.dk).

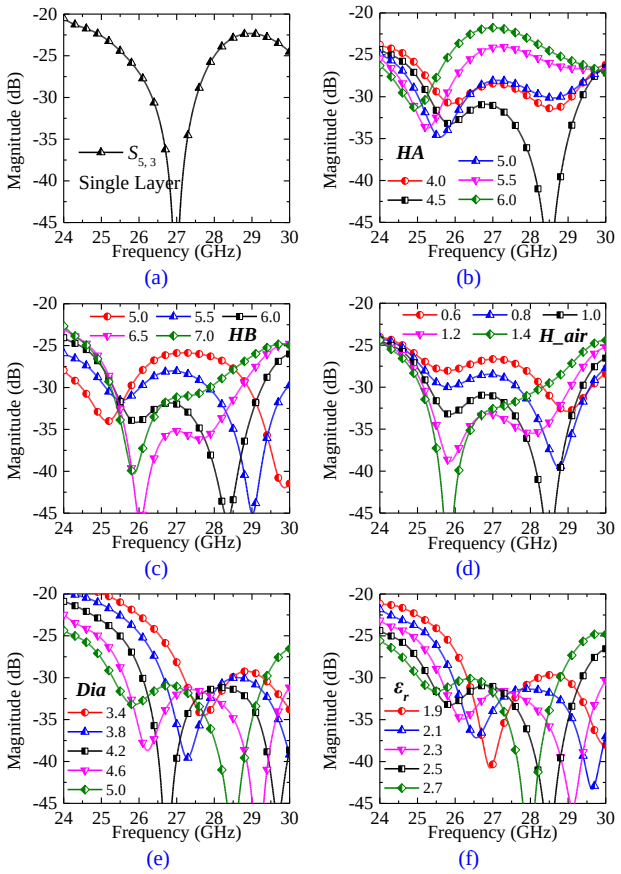

Fig. 2. (a) Simulated $S_{5,3}$ of the array with single-layer decoupling structure, where the diameter, the height, and the permittivity value of the dielectric stub are 4.0 mm, 5.5 mm, and 2.1, respectively. Simulated $S_{5,3}$ of the proposed one against different values of (b) *HA*, (c) *HB*, (d) *H_air*, (e) *Dia*, and (f) ε_r, where the common values are: *HA*=4.5 mm, *HB*=5.9 mm, *H_air*=1 mm, *Dia*=5.0 mm, and ε_r=2.1.

array integrated with single-layer dielectric stubs, where the mutual coupling can be suppressed, as discussed in [7]. Fig. 1(b) shows the array loaded with the proposed wideband decoupling structure, which is a dual-layer dielectric cylinder. Fig. 1(c) illustrates the MMW ±45° dual-polarized stacked patch antenna which is used as the antenna element, working from 24.0 GHz to 29.5 GHz. The thicknesses of the RO4450F layers are determined from bonding and impedance matching point of view. The bottom RO4350B layer is the substrate of the microstrip-line layer, whose thickness should be thin to avoid exciting higher modes with narrow line width. The physical dimensions are (mm): *L1*=5.08, *L2*=1.97, *L3*=6.57, *L4*=3.05, *LF*=0.95, *LT1*=1.72, *WT1*=0.41, *LT2*=1.71, *WT2*=0.36. Differential feeding is employed for each polarization to achieve high inner-port isolation and a symmetrical radiation pattern. The decoupling principle of the decoupled antenna array is simple. With the stubs, the electromagnetic field radiated by an element would be confined straight ahead of the radiating structure, while the waves propagating along the array aperture plane would be significantly reduced, as illustrated in Fig. 1(a). More importantly, compared to the one using a single-layer decoupling stub, the one with the dual-layer decoupling structure features a much wider decoupling bandwidth.

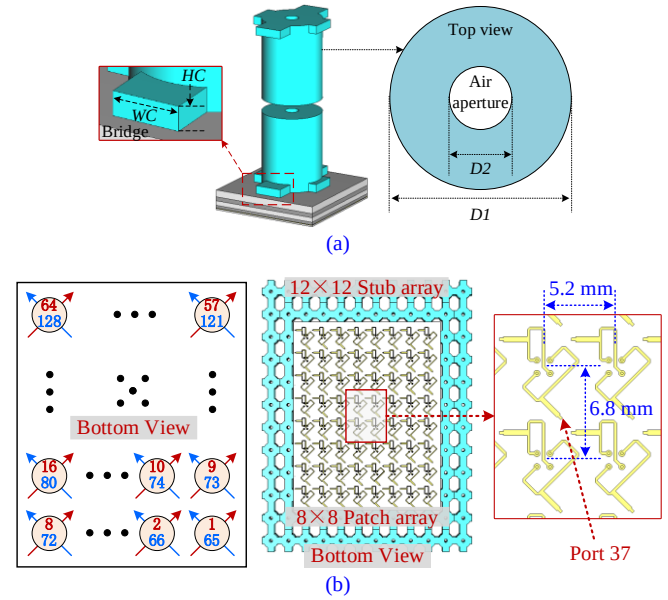

Fig. 3. (a) Configuration of the determined dual-layer decoupling structure. (b) Configuration of the 8×8 decoupled array and its port arrangement.

To explain the mechanism of the bandwidth improvement, parameter studies are provided, as shown in Fig. 2. Illustrated in Fig. 2(a) is the simulated $S_{5,3}$ of the array integrated with single-layer decoupling stubs. By properly selecting the diameter, height, and permittivity of the dielectric stub, the coupling between co-polarized adjacent elements would be well-suppressed at the center frequency. However, the coupling level is still higher than –25 dB when the frequency closes to 26/28 GHz. Figs. 2(b)-(f) illustrate the coupling levels between adjacent elements of the array integrated with the dual-layer decoupling stubs, against different dimensions of the stub and permittivity values of the dielectric material. It is seen that the proposed dual-layer decoupling stub enables a significant improvement in the decoupling bandwidth by introducing an additional decoupling resonance. The values of *HB*, *Dia*, and permittivity mainly determine the second decoupling frequency. By tuning the values of *HA* and *H_air*, the decoupling between the two resonances can be reduced to a low level. Finally, a wide decoupling bandwidth is enabled.

B. Design example

A design example is developed to show the performance of the proposed scheme. Based on the structures provided in Fig. 1, an 8×8 dual-polarized decoupled antenna array is established, as shown in Fig. 3. For ease of fabrication, small rectangular dielectric bridges are utilized to connect the stubs for array applications, as shown in the enlarged area in Fig. 3(a). The dielectric stub can be fabricated by 3D-printing technology, where the relative permittivity of the material is 2.65 in our lab. Note that the determined relative permittivity of the stub material is 2.1. Therefore, the decoupling dielectric stub is fabricated as a hollow cylinder, as shown in Fig. 3(a). The inner air aperture is employed for tunning the equivalent permittivity to the desired values of around 2.1. The optimized dimensions of the decoupling stub are (mm): *HA*=5.5, *HB*=5.9, *H_Air*=0.9, *HC*=0.6, *WC*=2.0, *D1*=4.4, *D2*=1.0. The

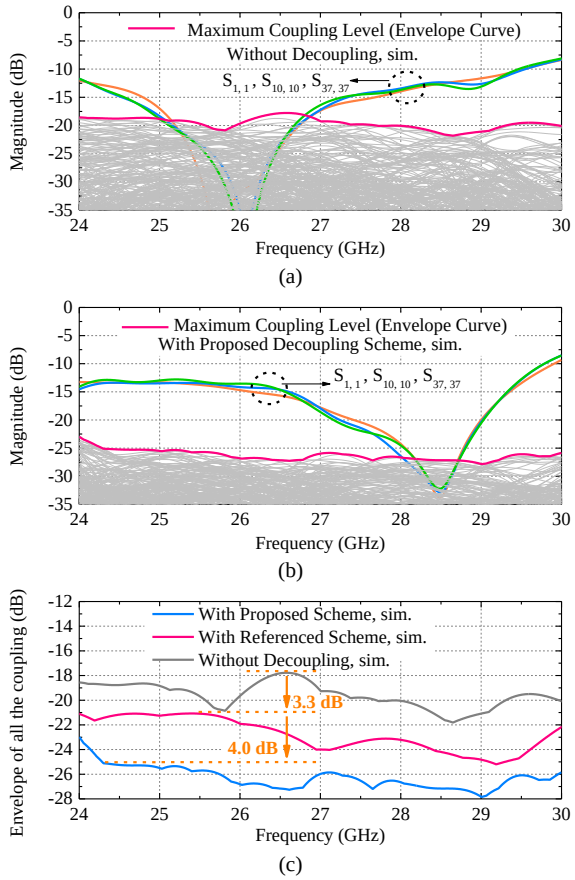

Fig. 4. Simulated *S* parameters of the array (a) without decoupling and (b) with the proposed decoupling scheme. (c) Coupling level comparison of the arrays without and with referenced [7] or proposed decoupling methods.

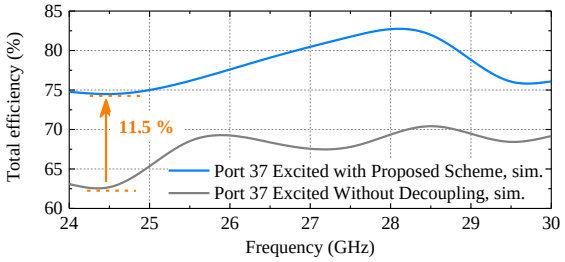

Fig. 5. Simulated total efficiencies of the arrays without and with the proposed scheme when Port 37 is excited.

center distances between elements in vertical and horizontal directions are 6.8 mm and 5.2 mm, respectively. To obtain a symmetrical electromagnetic environment, the decoupling part is set as a 12×12 stub array. The -45º and +45º polarized ports are set as Ports 1~64 and Ports 65~128, respectively, as shown in Fig. 3(b).

Further, full-wave simulations are carried out. The simulated *S* parameters are illustrated in Fig. 4, where Ports 1, 10, and 37 are chosen as the representative ports. For comparison purposes, the antenna arrays without decoupling and with the referenced decoupling scheme reported in [7] are also given. Please note that since the scheme in [7] was designed for Sub-6 GHz arrays without any discussions for MMW antennas, the results illustrated here are obtained from the 8×8 array consisting of the elements shown in Fig. 2 and the decoupling structure given in [7]. It is seen that the

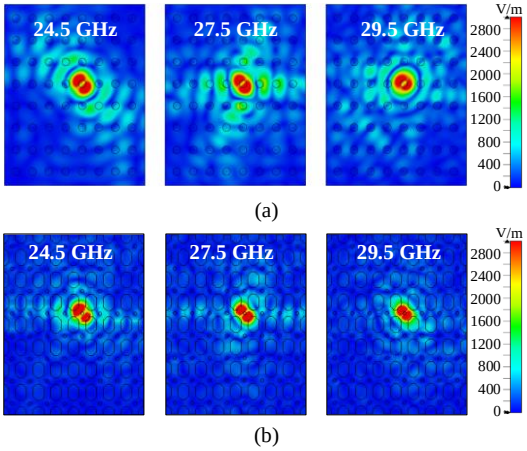

Fig. 6. Simulated E-field densities in front of the radiating aperture of the arrays (a) without decoupling and (b) with proposed decoupling structure when Port 37 is excited.

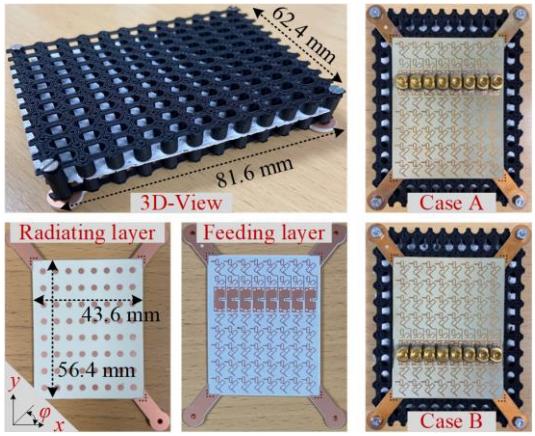

Fig. 7. Photos of the fabricated demonstrators, involving the 3D view of the decoupled array, top view of radiating and feeding layers, and the feeding of the two cases (Case A: ports 57~64, Case B: ports 33~40, as marked in Fig. 4(b)) soldered with MMPX connectors for measurement.

original array without decoupling features a strong coupling level whose maximum coupling is higher than -17.8 dB, which is significantly reduced to less than -25.1 dB within the band from 24.3 to 29.7 GHz. The coupling paths, including the leakage between adjacent, nonadjacent, co-polarized, and cross-polarized ports, are all well-suppressed. Fig. 4(c) is a comparison of the coupling level under different decoupling conditions. It is depicted that with the referenced decoupling structure given in [7], the isolation improvement is around 3.3 dB, while the one by using the proposed scheme is 7.7 dB within a wide frequency band.

The simulated total efficiency of the decoupled array is given in Fig. 5 when Port 37 is excited. Compared to the array without decoupling, the lowest total efficiency among the operating band is improved by 11.5%, from 62.5% to 74%. E-field density distribution in front of the radiating aperture is also provided, as illustrated in Fig. 6. It is verified that the proposed decoupling stub can greatly confine the electromagnetic waves propagating along the radiating aperture plane, as expected. Next, the developed 8×8 dual-polarized array is fabricated and measured.

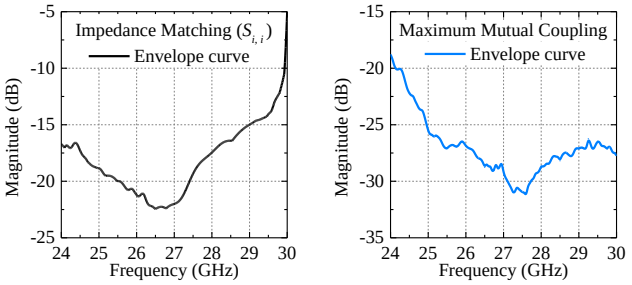

Fig. 8. Measured *S* parameters of the two demonstrators. (a) Impedance matching performance. (b) Maximum mutual coupling level.

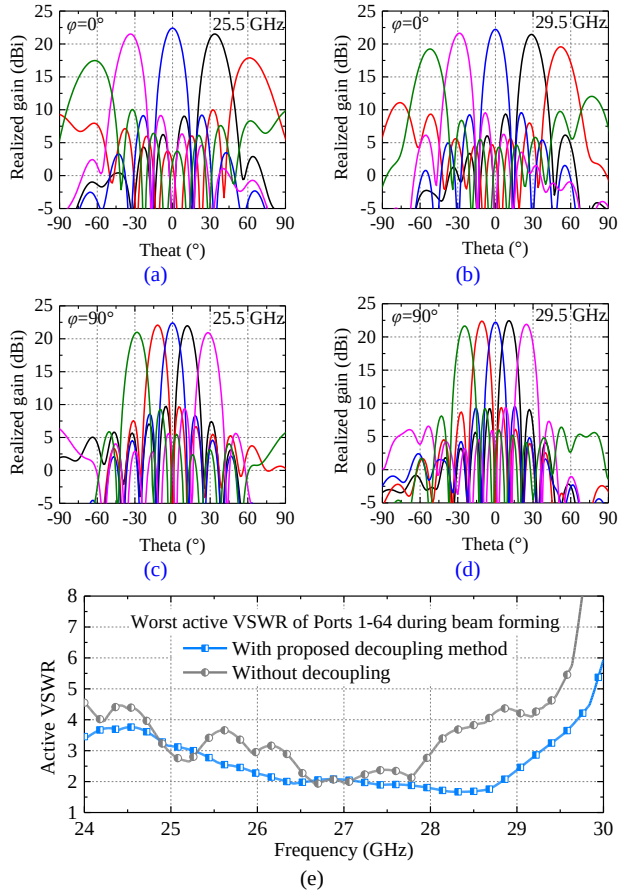

Fig. 9. Beam scanning performance when Ports 1-64 are excited, at (a) 25.5 GHz, φ=0°, (b) 29.5 GHz, φ=0°, (c) 25.5 GHz, φ=90°, (d) 29.5 GHz, φ=90°. (e) Worst active VSWR of Ports 1-64 during beam forming of the arrays with and without decoupling.

III. MEASUREMENT

The photos of the fabricated decoupled 8×8 antenna array are given in Fig. 7. The entire size of the array is 81.6 × 62.4 × 13.822 mm^3. To solder the MMPX connectors for measurements, two cases (marked as Cases A and B), corresponding ports 57~64 and ports 33~40 correspondingly, are selected as the study cases.

The measured *S* parameters of the two cases are illustrated in Fig. 8. All the element ports are well-matched, and the impedance bandwidth is over 6 GHz from less than 24 GHz to 29.9 GHz, referring to $|S_{i,i}| \leq -10$ dB. The mutual coupling between adjacent elements and between non-adjacent elements are almost less than -25 dB, except slight fluctuations around 24.5 GHz. Owing to the limited physical space at the feeding layer, the ports except the selected row are open-circuited during testing. We have checked that the decoupled array with open-circuited ports features similar decoupling and matching responses to the one with terminated ports through full-wave simulations. The basic requirements for the scanning angles are ±60º and ±30º at azimuth and elevation directions, respectively. The side lobe level for 60º scanning is around 12 dBi and 7 dB lower than that of the main beam, which is acceptable. The simulated beam-scanning performance of the decoupled array at φ=0º and φ=90º planes are shown in Figs. 9(a)-(d), where Ports 1-64 are excited with different phase settings. The active impedance-matching performance of Ports 1-64 during beam scanning is provided, as shown in Fig. 9(e). Some results of the coupled array are also given. It is seen that the decoupled array features a better active impedance matching performance within a wide frequency range, compared to the coupled array.

Table I Comparison between the proposed decoupled antenna and recently published decoupled antennas

Reference /Year	Array configuration	Operating band Bandwidth	Element distance*	Isolation level
[1]/2017	2×2 Dual-polarized	3.3~3.8 GHz 14.1%	0.57λ_{up} (H) 0.75λ_{up} (V)	25 dB
[7]/2021	4×4 Dual-polarized	4.4~5.0 GHz 12.8%	0.52λ_{up}	25 dB
[11]/2021	4×4 Single-polarized	24.5~29.5 GHz 18.5%	0.44λ_{up} (H) 0.86λ_{up} (V)	20 dB
[14]/2022	1×4 Single-polarized	25.5~26.5 GHz 4.0%	0.49λ_{up}	35 dB
This work	8×8 Dual-polarized	24.9~29.9 GHz 18.2%	0.52λ_{up} (H) 0.68λ_{up} (V)	25 dB

*Referring to the upper edge of the operating band.

Some recently published decoupling methods are summarized in Table I for comparison purposes, where an isolation level of around 25 dB is selected as the reference value. The operating bandwidth (the common band of the decoupling and impedance matching) of the proposed one is over 18%. Although the work reported in [11] features a wider bandwidth, the referred isolation level is 20 dB, with a larger element distance. The work provided in [14] achieved a higher isolation of 35 dB, at the cost of a narrow bandwidth. Besides, the proposed one enables the decoupling of dual-polarized antenna arrays. This was not mentioned in the published decoupling methods for millimeter-wave antennas.

IV. CONCLUSION

To reduce the strong mutual coupling among elements in MMW large-scale antenna arrays, a wide-band decoupling structure is proposed by developing a dual-layer dielectric structure loaded in front of the array aperture. Compared to the recently published decoupling methods for MMW antennas, the proposed scheme features a simple design procedure, wide operating band, low insertion loss, as well as good effectivity for dual-polarized array configuration, making it attractive for large-scale antenna arrays in 5G and beyond systems.

REFERENCES

[1] K. -L. Wu, C. Wei, X. Mei and Z. -Y. Zhang, "Array-Antenna Decoupling Surface," *IEEE Transactions on Antennas and Propagation*, vol. 65, no. 12, pp. 6728-6738, Dec. 2017.

[2] Y. -M. Zhang, S. Zhang, J. -L. Li and G. F. Pedersen, "A Transmission-Line-Based Decoupling Method for MIMO Antenna Arrays," *IEEE Transactions on Antennas and Propagation*, vol. 67, no. 5, pp. 3117-3131, May 2019.

[3] Y. -F. Cheng and K. -K. M. Cheng, "Compact Wideband Decoupling and Matching Network Design for Dual-Antenna Array," *IEEE Antennas and Wireless Propagation Letters*, vol. 19, no. 5, pp. 791-795, May 2020.

[4] Y. -M. Zhang and S. Zhang, "A Side-Loaded-Metal Decoupling Method for 2 × N Patch Antenna Arrays," *IEEE Antennas and Wireless Propagation Letters*, vol. 20, no. 5, pp. 668-672, May 2021.

[5] M. Li, M. Wang, L. Jiang and L. K. Yeung, "Decoupling of Antennas With Adjacent Frequency Bands Using Cascaded Decoupling Network," *IEEE Transactions on Antennas and Propagation*, vol. 69, no. 2, pp. 1173-1178, Feb. 2021.

[6] Y. -M. Zhang and S. Zhang, "A Novel Aperture-Loaded Decoupling Concept for Patch Antenna Arrays," *IEEE Transactions on Microwave Theory and Techniques*, vol. 69, no. 9, pp. 4272-4283, Sept. 2021.

[7] P. Mei, Y. -M. Zhang and S. Zhang, "Decoupling of a Wideband Dual-Polarized Large-Scale Antenna Array With Dielectric Stubs," *IEEE Transactions on Vehicular Technology*, vol. 70, no. 8, pp. 7363-7374, Aug. 2021.

[8] M. Li, Y. Zhang, D. Wu, K. L. Yeung, L. Jiang and R. Murch, "Decoupling and Matching Network for Dual-Band MIMO Antennas," *IEEE Transactions on Antennas and Propagation*, vol. 70, no. 3, pp. 1764-1775, March 2022.

[9] Y. Li and Q. -X. Chu, "Self-Decoupled Dual-Band Shared-Aperture Base Station Antenna Array," *IEEE Transactions on Antennas and Propagation*, vol. 70, no. 7, pp. 6024-6029, July 2022.

[10] Y. M. Pan, X. Qin, Y. X. Sun and S. Y. Zheng, "A Simple Decoupling Method for 5G Millimeter-Wave MIMO Dielectric Resonator Antennas," *IEEE Transactions on Antennas and Propagation*, vol. 67, no. 4, pp. 2224-2234, April 2019.

[11] X. Ai, Y. Liu, Y. Jia and Y. Xu, "4×4 Antenna Array for 5G Millimeter Wave Applications," *2021 International Conference on Microwave and Millimeter Wave Technology (ICMMT)*, Nanjing, China, 2021, pp. 1-3.

[12] X. Wu, Z. Chen, T. Yuan and S. Liu, "A Decoupling Method for E-Plane Coupled Millimeter-Wave MIMO Dielectric Resonator Antennas," *2021 Cross Strait Radio Science and Wireless Technology Conference (CSRSWTC)*, Shenzhen, China, 2021, pp. 109-111.

[13] D. A. Sehrai et al., "Metasurface-Based Wideband MIMO Antenna for 5G Millimeter-Wave Systems," *IEEE Access*, vol. 9, pp. 125348-125357, 2021.

[14] W. Song, X. -W. Zhu, L. Wang and W. Hong, "Simple Structure E-plane Decoupled Millimeter Wave Antenna Based on Current Cancellation Model," *IEEE Transactions on Antennas and Propagation*, vol. 70, no. 10, pp. 2224-2234,